1) Project Information

Title: Dual Assimilation of Microwave and Thermal-Infrared Observations of Soil Moisture into NLDAS for Improved Drought Monitoring

PI: Xiwu Zhan, NESDIS, NOAA
Co-PI: Christopher Hain, Earth System Science Interdisciplinary Center, U. of Maryland
Co-PI: Martha Anderson, HRSL, USDA-ARS
Co-I: Mark Svoboda, NDMC, U. of Nebraska-Lincoln
Co-I: Brian Wardlow, NDMC, U. of Nebraska-Lincoln
Co-I: Michael Ek, NCEP, NOAA
Co-I: Wade Crow, HRSL, USDA-ARS
Collaborator: John Mecikalski, UAH
Collaborator: William Kusatas, HRSL, USDA-ARS

2) Results and Accomplishments

The objective of this project is to produce a real-time data assimilation (DA) system for optimal assimilation of thermal infrared (TIR) and microwave (MV) soil moisture (SM) and insertion of near real-time green vegetation fraction (GVF) into the Noah land-surface model component of the National Land Data Assimilation System (NLDAS) using the NASA Land Information System (LIS). NLDAS produces the hydrologic products (e.g. soil moisture, evapotranspiration, and runoff) used by NCEP for operational drought monitoring, but these products are sensitive to model input errors in soil texture (affecting infiltration rates and water holding capacity) and prescribed precipitation rates. Periodic updates of SM state variables in LSMs achieved by assimilating diagnostic moisture information retrieved using satellite remote sensing have been shown to compensate for model errors and result in improved hydrologic output. Assimilation results will be validated using in-situ SM observations and a data denial validation methodology. Additionally, an extensive quantitative evaluation of SM moisture anomalies from the DA simulations will be compared to ALEXI ESI and standard drought metrics, including the operational NLDAS output. Outputs from the real-time DA system will include near real-time (updated each night) maps of surface and root-zone SM, ET and runoff and will be delivered to the Climate Prediction Center for use in the North American Drought Briefing and to the National Drought Mitigation Center in support of the United States Drought Monitor.

a. Assessment and Optimization of Data Assimilation Methodology

The data assimilation methodology required a number of datasets to be processed and archived for the retrospective period 2000-2014. These datasets include:

- NLDAS forcing, used for initializing and for providing meteorological forcing for the Noah LST.

- TRMM 3B42RT precipitation estimates, used for providing precipitation input for the open-loop simulation and each data assimilation simulation in the data denial validation methodology.
- NESDIS green vegetation fraction and MODIS leaf area index, is used to update the fraction of green vegetation in the Noah LSM.
- ALEXI soil moisture retrievals (thermal-infrared), used in the data assimilation experiments.
- LPRM (AMSR-E) passive soil moisture retrievals and the ESA Essential Climate Variable (ECV) merged active + passive microwave soil moisture dataset.

Comparison of NESDIS GVF vs. MODIS LAI

The impact of updating the fraction of green vegetation parameter in the Noah LSM will be quantified in a series of data assimilation experiments, as compared to the climatological specification that is currently used in NLDAS. Currently, two widely used GVF datasets are available: (1) the NESDIS Green Vegetation Fraction dataset, based on a scaling of minimum and maximum NDVI and (2) the MODIS Leaf Area Index dataset, which can be converted to a fraction of green vegetation based on a canopy gap fraction methodology. In general, the NESDIS product seems to overestimate green vegetation fraction of agricultural regions and dense forests where saturation of the NDVI signal occurs. Therefore, a final decision to use fraction of green vegetation from MODIS was made to maintain consistency between the data assimilation simulations and the dataset used in the processing and subsequent retrieval of soil moisture from ALEXI. The next step was to compare the near-real-time MODIS LAI product (used to compute green vegetation cover) against the climatological fields currently used in the Noah LSM. These climatological fields are based on a similar NDVI scaling routine as used in the NESDIS GVF product. Additionally, the climatological fields are based on a relatively short record 5-year period. For applications pertaining to drought monitoring, the use of climatological vegetation fields in Noah can cause large differences in the observed vegetative state and the climatological fields. Fig. 1 shows the importance of using near-real-time vegetation data in Noah, in the example shown; the anomalies in GVF for 5 August 2012 were on the order of 10 to 20% below normal over the central US in drought affected areas.

Re-scaling/interpolation of ALEXI and LPRM moisture retrievals

Soil moisture retrieval datasets and SM predictions from LSMs can exhibit significant differences in their climatological statistics. The effect of these biases can be mitigated by employing a technique using the first two statistical moments (mean and variance) to rescale ALEXI and LPRM soil moisture retrievals. ALEXI soil moisture is retrieved once per day in cloud-free pixels over CONUS at a spatial resolution of 10 km, while LPRM soil moisture is available at a spatial resolution of 25 km. Each soil moisture dataset was spatially interpolated to the 0.125° NLDAS domain. Dataset-specific values of climatological means (μ) and variances (σ) for each day of the year are calculated for all three datasets based on a 28-day centered moving sampling window and all years of ALEXI and LPRM retrievals. Using these statistics, SM retrievals from remote sensing sources (ALEXI and LPRM) are linearly re-scaled to provide a volumetric SM estimate consistent with Noah.

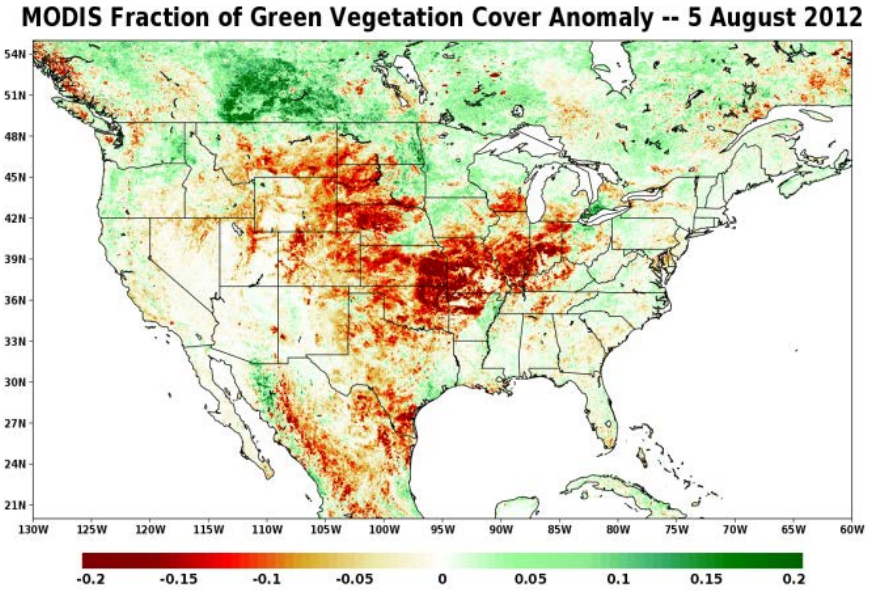

Figure 1. MODIS fraction of green vegetation cover anomaly for 5 August 2012 (anomaly calculated over MODIS period of record [2000-2014]).

The initial evaluation of the data assimilation experiments using climatological green vegetation fraction has shown a successful assimilation of ALEXI and LPRM soil moisture. The following summarize the initial evaluation of the results based on the data denial evaluation methodology:

- On average, all three of the assimilation strategies (TIR; MW; TIR+MW) reduce the RMSD with respect to the CONTROL case in comparison with the OLP simulation.
- Spatially averaged RMSD for the 0-5 cm Noah soil moisture layer, valid during all warm season months (April-October), for the OLP, ALEXI, LPRM and DUAL cases are 0.046 $m^3 m^{-3}$, 0.032 $m^3 m^{-3}$ (30% reduction), 0.030 $m^3 m^{-3}$ (35% reduction), and 0.028 $m^3 m^{-3}$(39% reduction), respectively.
- The magnitude of RMSD improvement (in terms of % improvement) in the root-zone layer is similar in all cases compared to that in the surface layer: RMSD for the OLP, ALEXI, LPRM and DUAL cases are 0.041 $m^3 m^{-3}$, 0.028 $m^3 m^{-3}$ (32% reduction), 0.034 $m^3 m^{-3}$ (17% reduction), and 0.033 $m^3 m^{-3}$ (20% reduction), respectively.
- A majority of the study domain exhibits improvement greater than 0.01 $m^3 m^{-3}$ relative to the OLP simulation in the surface layer, regions of the eastern CONUS exhibit no significant improvement and/or degradation (e.g., RMSD differences between -0.01 $m^3 m^{-3}$ and 0.01 $m^3 m^{-3}$).
- In general, spatial patterns in root-zone SM (5-100 cm) improvement are similar to those for the surface layer over a majority of the central CONUS, with widespread improvement on the order of 0.01 to 0.03 $m^3 m^{-3}$, however more significant differences are observed over the western CONUS.

b. Improvements to the ALEXI ESI and Soil Moisture Proxy Dataset and Transition from AMSR-E based MW SM Products

Transition from 10-km Products to 4-km Products over CONUS

To better exploit the full resolution of GOES Imager thermal data (4-km at nadir) all CONUS ALEXI ESI and SM datasets were transitioned from 10-km GOES Sounder thermal data to 4-km GOES Imager thermal data. The higher resolution products provide better spatial detail in the ESI and SM datasets, especially in regions with significant gradients. Fig. 2 shows an example of original 10-km ESI product for August 7, 2007 and of the new 4-km ESI product for the same date. All near-real-time ALEXI ESI and SM products are now available at the updated 4-km resolution. Additionally, the entire ALEXI climatology (back to 2000) was reprocessed at the new resolution to be consistent with the near-real-time products.

Transition from LPRM AMSR-E MW SM products to ESA ECV Merged Active+Passive MW SM Products

During 2011, the AMSR-E sensor which was the source of passive microwave soil moisture retrievals used in this study failed. Our research team investigated several other microwave-based soil moisture datasets to use as a replacement for the AMSR-E-based LPRM products that were initially used. The team decided to transition the analysis to the ESA Essential Climate Variable (ECV) merged active and passive soil moisture dataset. The ESA ECV datasets is the most complete and consistent global microwave soil moisture dataset and extends back to 1978 at a spatial resolution of 0.25 deg. The dataset uses observations from a series of sensors: C-band scatterometers (ERS-1/2 scatterometer, METOP Advanced Scatterometer [ASCAT]) and multi-frequency radiometers (SMMR, SSM/I, TMI, AMSR-E, Windsat).

c. Intercomparison of ALEXI, ECV and Noah Soil Moisture for Improved Retrieval Error Characterization

SM Anomaly Correlation Analysis

In this section, Noah SM predictions are used as the baseline to evaluate the relative performance of satellite-based SM retrievals from either TIR or MW observations. Figure 3 (a-d) presents the anomaly correlations between each of the satellite based SM products (ALEXI, ECV, ECV-active, and ECV-passive) and Noah SM predictions over the validation period of 2000 – 2013. The sample size at each pixel is presented in Figure 3e. The differences in anomaly correlation with respect to ALEXI, ECV, ECV-active and ECV-passive products are shown in Figure 4, from which their relative skills can be compared. The average correlation coefficients for each of the product over the land pixels of CONUS domain is listed in Fig. 3, along with the statistics of the number of pixels (in percentage) with the highest anomaly correlation compared to the others.

In general, the satellite-based SM products agree well with the Noah LSM predictions, especially over the central United States. Among all the satellite based SM products, ALEXI presents best agreement with Noah predictions with the correlation of 0.52 averagely over the CONUS. The correlation map of ALEXI product exhibits overall positive correspondence without regions with significant low or negative correlations. The anomaly correlation of ECV-passive retrievals turns out to be the weakest, with low correlation over the majority of eastern area and over the west coast of the US. It is interesting to notice that the ECV-active and ECV-passive products provide complementary information with respect to SM anomalies, the former with better consistency over eastern region with moderate vegetation density but the latter over western area with low

vegetation cover. ECV-merged makes fully use of the strengths from both active and passive sensors in term of their sensitivities to land vegetation density, and therefore, SM anomalies of the ECV-merged product match well with Noah SM predictions across CONUS with the mean correlation coefficient of 0.49 over all land pixels, larger than either of the individual products. In the central US, where both individual products (ECV-active and ECV-passive) correlate well, ECV merged product takes the average of both individual products which lead to the anomaly correlation of ECV merged product not as strong as either ECV_ACT or ECV_PAS. Also, the relatively low correlation can be detected along the border of California and Nevada in the anomaly correlation map of ECV merged product.

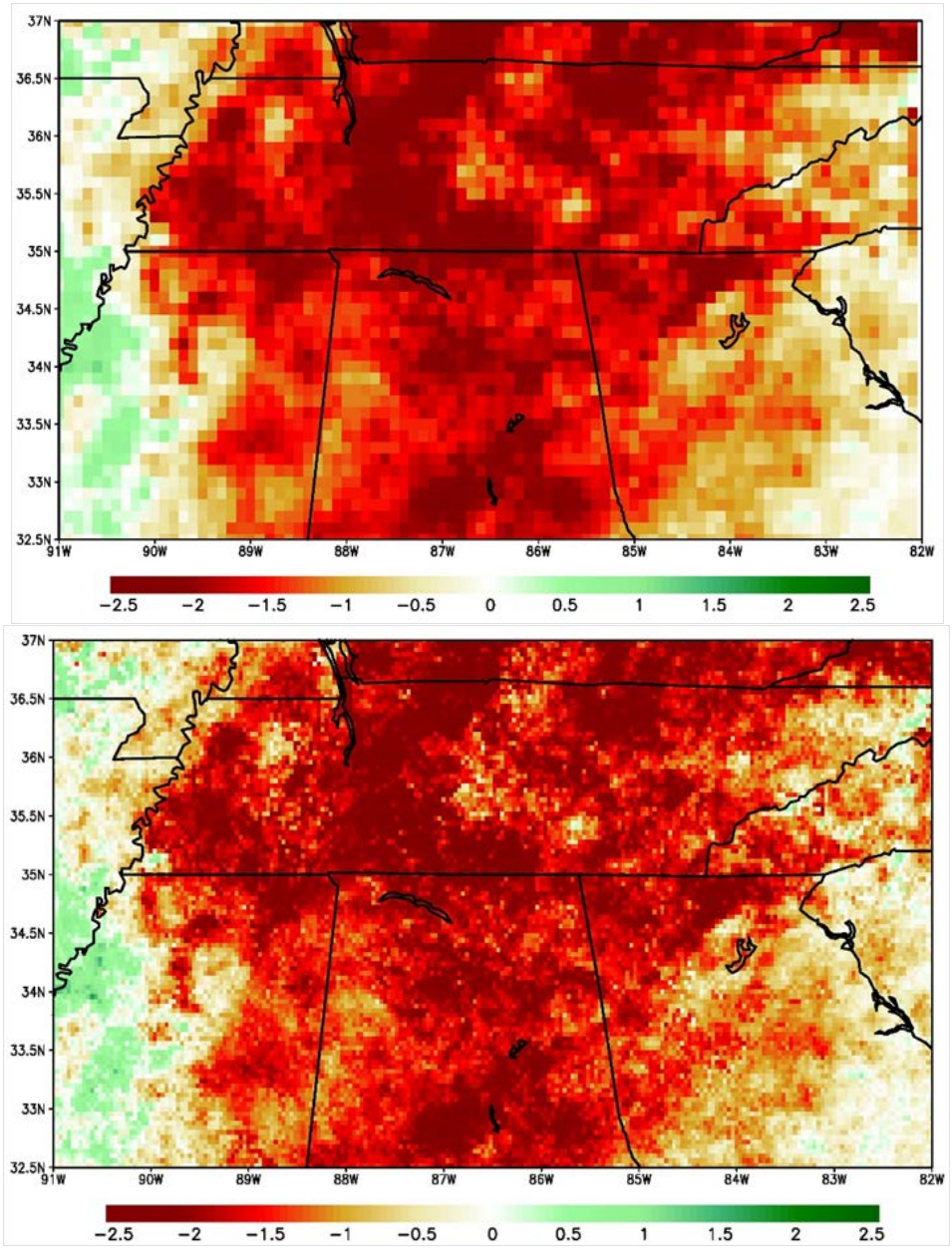

Fig 2. ALEXI ESI for 7 August 2007 from the original 10-km domain (top) and the new updated 4-km domain (bottom).

Land surface vegetation cover is found to be a key factor to interpret the retrieval accuracy of WM satellite based products. The correlation map of ECV passive present a similar pattern with the multiyear (2000 - 2013) average vegetation fraction cover map. The relative performance between the active and passive is better illustrated in the correlation difference map shown in Fig. 4d. For ECV-passive, better consistency can be found in the regions with low vegetation cover (western and central US), while the correspondence is low over relatively dense vegetation covers (high terrain of western US and eastern US). On the other hand, the ECV-active product presents complementary performance with relatively high correlations over the moderate or dense vegetation pixels, but performs poorly over desert areas. Notably, ALEXI retrievals performs best in the high vegetation fraction areas, while MW-based products are better representative over the desert regions (passive) and central US (active and passive) where average vegetation fraction is low. ECV-active retrievals show poor correspondence over the western US, where surface roughness is another sensitive factor to active MW sensors.

Comparison with In-situ SM from the North American Soil Moisture Database (NASMD)

The SM anomalies from satellite and model based products are evaluated with the SM anomalies observed from nearly five hundred North American Soil Moisture Database (NASMD) sites. The two-pair t-test is applied to test statistical significance of the anomaly correlations at the 99% confidence level. The passing rates of the anomaly correlations of satellite-based SM products are between about 70% and 93.7%. Listed in Fig. 5 are the average correlations for each of the SM products when statistics are statistically significant for all involved products at 459 ground sites in total. The spatial distributions of time series anomaly correlations between each of the SM products (satellite based products and Noah predictions) and ground observations are also shown in Fig. 5. The distribution maps of anomaly correlation illustrate that all products performed well in the central and eastern United States, while the correlations tend to be relatively lower in the western area for MW-based SM products (especially in regions of complex terrain). Noah predictions present the highest mean anomaly correlation of 0.51 relative to the ground validation dataset. Except for a small amount of validation sites in Oregon, the anomaly correlations of Noah predictions are strongly correlated with ground observations with the correlation coefficients on the order of 0.5 to 0.8. The satellite based products are also considerably skillful with respect to the representativeness of anomalies in soil moisure. ALEXI SM anomalies show good correspondence with the ground observations with a mean anomaly correlation coefficient of 0.40, identical to that found with the merged ECV product and ECV active product.

Since vegetation density is found to be a key factor to satellite signals for both MW and TIR sensors, time series anomaly correlations are computed as the function of average vegetation fraction cover. Noah LSM performs well in a wide range of vegetation conditions. The histogram of ALEXI and ECV-merged have the similar distribution as that of Noah SM anomalies, but their correspondence strength is slightly less than that of Noah LSM estimates. It indicates that the ALEXI and ECV-merged products are also considerably representative over various levels of vegetation covers. However, the performance of ECV-passive is limited when vegetation fraction cover goes is higher than 0.6, while that of ECV-active is poor over low vegetation cover regions (fraction cover less than 0.15).

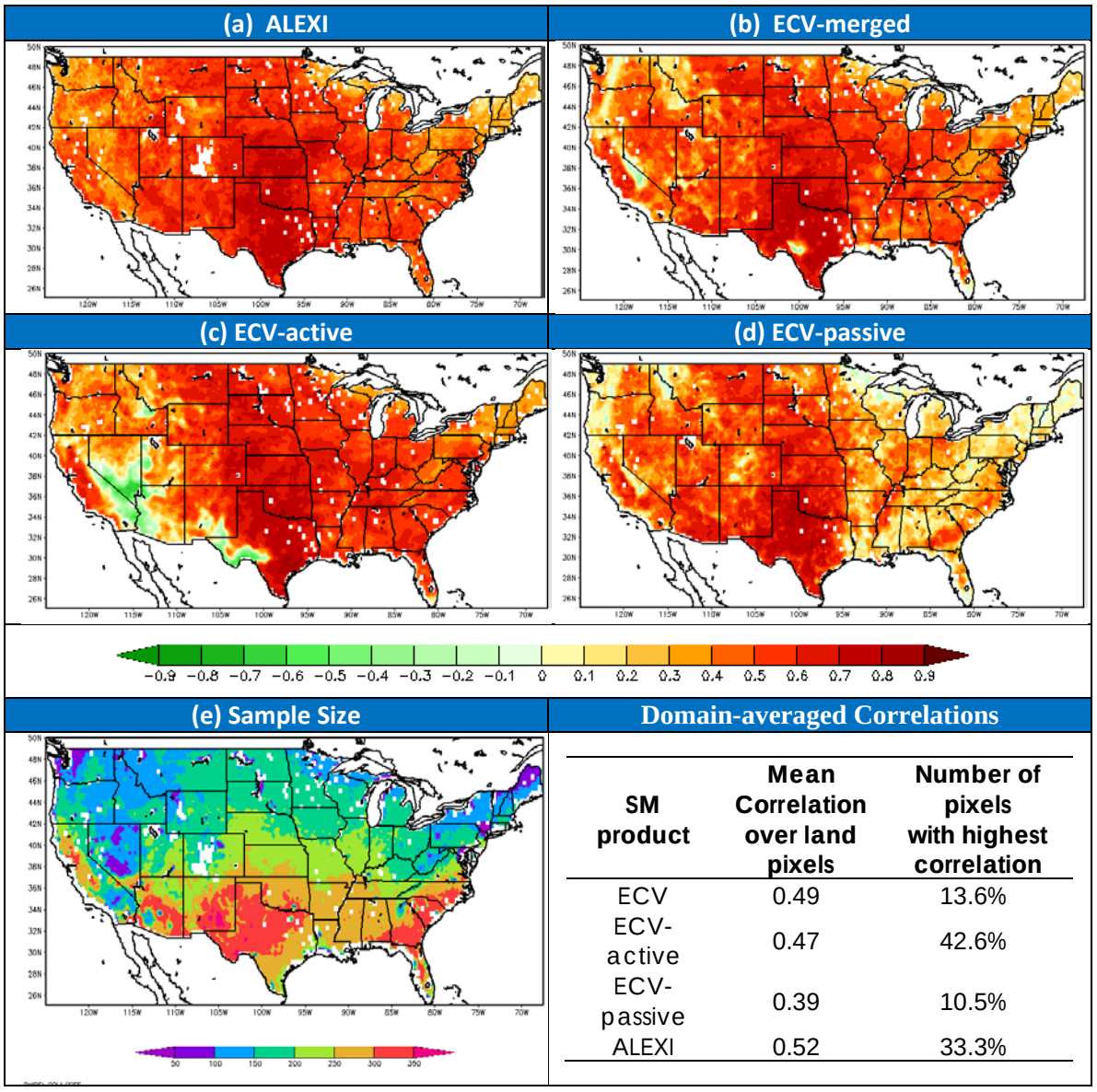

Domain-averaged Correlations

SM product	Mean Correlation over land pixels	Number of pixels with highest correlation
ECV	0.49	13.6%
ECV-active	0.47	42.6%
ECV-passive	0.39	10.5%
ALEXI	0.52	33.3%

Fig. 3. Anomaly correlations computed between satellite-based SM products (ECV-merged, ECV-active, EC-passive and ALEXI) and Noah SM predictions over the period of 2000 – 2013 (a-d); and analysis sample size (e).

Quantifying the impact of non-precipitation water sources (e.g., irrigation, groundwater) on ALEXI and Noah estimates of ET

Traditional soil water balance modeling is based on one-dimensional (vertical-only) water flow, free drainage at the bottom of the soil column, and neglecting ancillary water inputs due to processes such as irrigation. As a consequence, the vertical infiltration of local precipitation represents the only source of soil water available for surface evapotranspiration (ET). However, recent work has also highlighted the importance of secondary water source (e.g., irrigation, groundwater extraction, inland wetlands and the lateral redistribution of water by topography)

and sink (e.g., tile drainage in agricultural areas) processes on the partitioning of evaporative and sensible heat fluxes at the land surface. While attempts have been made to incorporate irrigation tile drainage (and groundwater processes into land surface models (LSMs), these efforts generally require parameters that are difficult to measure (e.g., the volume of water applied in irrigation or groundwater recharge rates) and modify LSM outputs in ways that are challenging to validate. Surface energy balance models based on thermal infrared remote sensing offer a top-down opportunity to directly observe the impact of non-precipitation water sources and anthropogenic water sinks on the land surface energy balance. For example, ALEXI uses time-differential measurements of morning land surface temperature (LST) rise to diagnose the partitioning of available energy into sensible, latent and ground heat flux components. In contrast to prognostic LSMs, ALEXI does not employ a water balance model to predict ET and soil water availability. Instead, water availability and its subsequent impact on surface energy fluxes is diagnosed directly from the observed pre-noon rise in LST. As a result, the model requires no *a priori* parameterization of water source and/or sinks processes. Therefore, understanding the effects of these non-precipitation inputs on diagnostic methods, such as ALEXI, and prognostic methods, such as LSMs [e.g., Noah] is becoming increasingly important, especially in drought monitoring applications. For example, regions where large precipitation deficits are observed, yet other sources of soil moisture are available (e.g., irrigation or vegetation tied to groundwater reserves) could lead to divergent anomaly signatures from the two methods during drought periods.

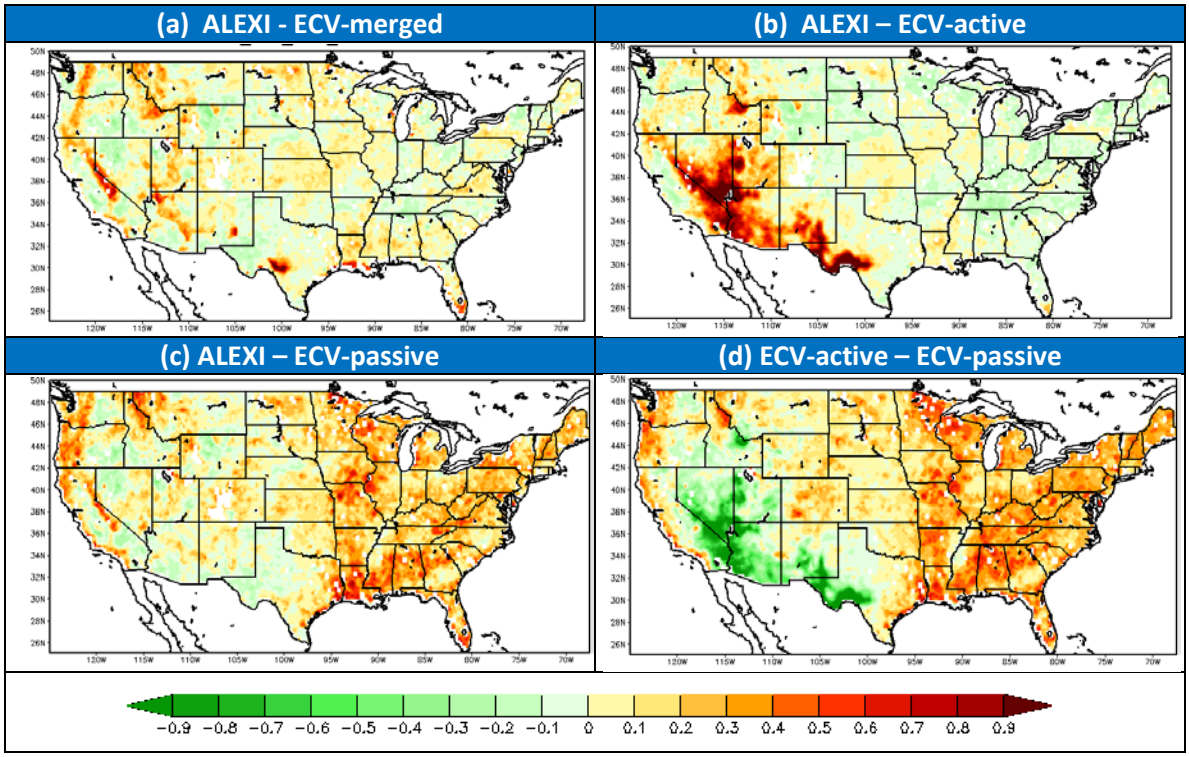

Fig. 4. Difference in anomaly correlations computed between (a) ALEXI and ECV-merged, (b) ALEXI and ECV-active, (c) ALEXI and ECV-passive and (d) ECV-active and ECV-passive.

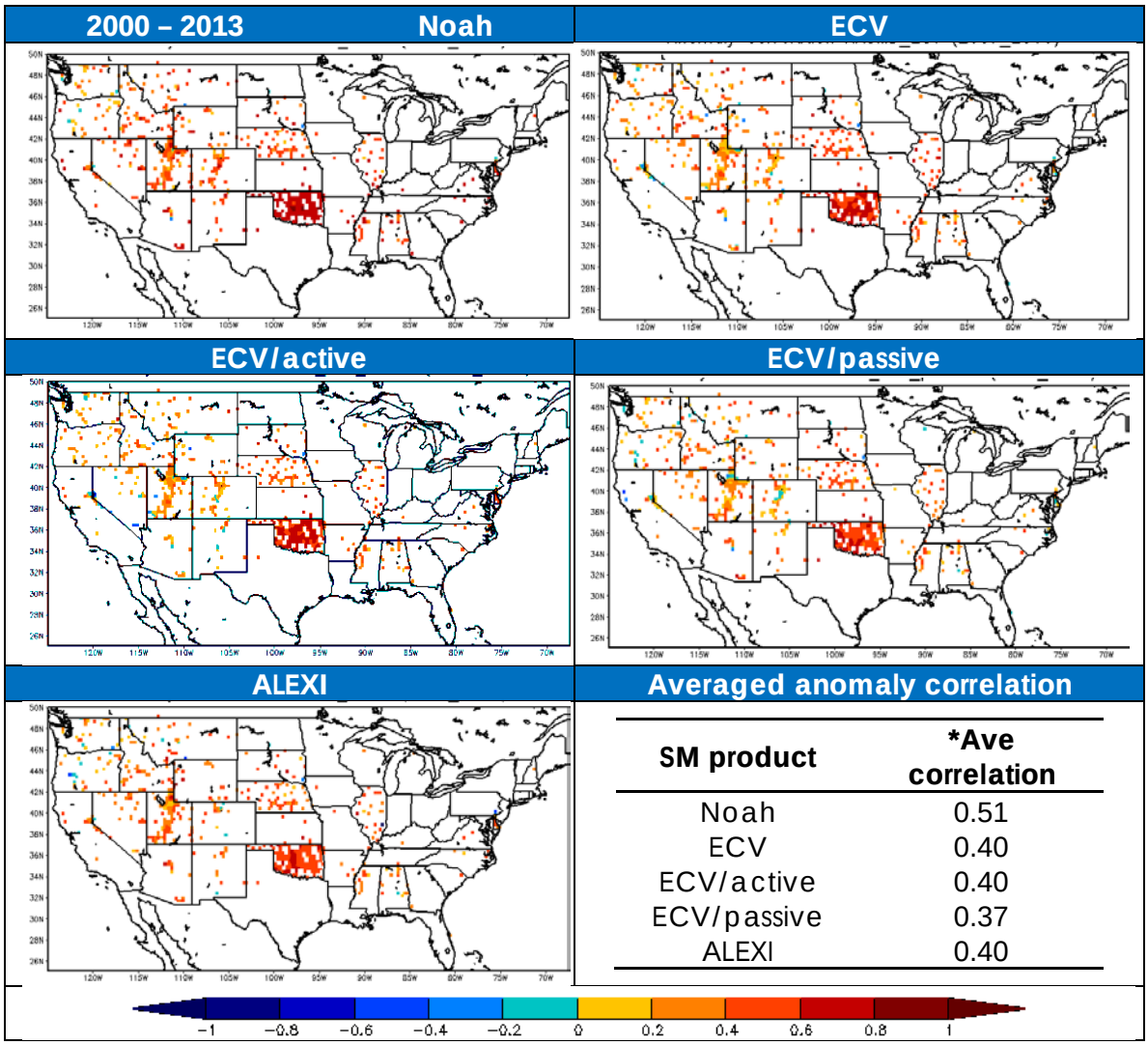

Fig. 5. Time series anomaly correlation coefficients computed between SM products (Noah, ECV, ECV/active, ECV/passive and ALEXI) and ground observations over the period of 2000 – 2013.

Since the standard Noah formulation lacks the ability to represent any water source except local precipitation, areas with large irrigation and/or groundwater-based water inputs should demonstrate a negative bias in LE_{NOAH} relative to LE_{ALEXI}. Likewise, these same areas should also be associated with relatively low VAR_{ALEXI} (since effects of inter-annual precipitation variability will be largely muted by irrigation and/or groundwater extraction). Conversely, areas in which Noah simulations neglect the impact of tile drainage (i.e., anthropogenic sinks) should be associated with a positive bias in LE_{NOAH} relative to LE_{ALEXI}. This unit-less index can be interpreted as a qualitative indicator of the impact of non-precipitation water sources on the diagnostic energy balance model output. In particular, large positive ASSET values reflect regions where the neglect of non-parameterized moisture *sources* (e.g., irrigation, extraction of shallow groundwater by phreatophytic plants or soil wicking, or direct evaporation from surface water) introduces a negative bias in growing-season LE_{NOAH} results. Conversely, negative ASSET values will reflect regions where *sinks* in soil moisture (e.g., tile drainage) are not

accurately represented in the Noah LSM, leading to a positive bias in seasonal LE_{NOAH}.
Fig. 6 maps unit-less 4-km ASSET index values over the CONUS domain. Pixels where non-precipitation moisture inputs may have a significant effect on clear-sky LE (areas of elevated LE_{ALEXI} as compared to LE_{NOAH} and low VAR_{ALEXI}) are denoted as positive values (green and blue tones). Conversely, negative ASSET values (red tones) potentially reflect the neglect of anthropogenic sinks in Noah surface energy balance predictions. As discussed above, areas of complex terrain are masked and shaded in grey. Spatial variations in positive ASSET values appear to accurately map the extent and the magnitude of non-precipitation water sources (e.g., irrigation; shallow water table depths; surface wetlands) on the surface energy balance. Labeled domains in Fig. 6 correspond to areas examined in detail below: (*i*) irrigated agricultural regions of the western CONUS (e.g., the Central Valley of California, Snake River Valley of southern Idaho, central Washington and south of the Salton Sea in extreme southern California); (*ii*) irrigated agricultural regions in the south central US (e.g., regions in the panhandle of Texas, western Kansas and large portions of Nebraska); (*iii*) the north central US exhibiting numerous soil water sources (e.g., shallow water table and surface wetlands (prairie potholes) and sinks (e.g., extensive agricultural tile drainage)), and (*iv*) the southeastern US, a region with extensive irrigation and shallow water tables in the Mississippi River valley, extensive wetlands along the Gulf Coast and shallow water table throughout much of Florida. Large positive ASSET values in many of these areas can generally be explained via comparisons to independent irrigation and/or groundwater depth maps shown in Figs. 6b and 6c. Likewise, the occurrence of negative ASSET values in the north-central US may be partially attributed to the known impact of agricultural tile drains

d. Improved Drought Monitoring based on assimilation for TIR and MW SM Products into the Noah LSM

i. Noah / ALEXI / LPRM (2003-2011)

A preliminary analysis of the simulations which assimilated ALEXI and LPRM SM retrievals were compared to USDM classifications (and anomalies) and SM anomalies from the Control simulation (Noah with no assimilation forcing with NLDAS precipitation; Fig. 2). Spatial anomaly correlations were computed for the following simulations against anomalies in the USDM classifications to assess how the assimilation of ALEXI and LPRM improved the representation of drought in the USDM. The anomaly correlations were computed over the 2003- 2011 analysis period for the months of June, July and August (consistent with LPRM availability; however additional analysis were performed for ALEXI which is available during the entire 2000-2011 periods). Spatial anomaly correlations for raw ESI (ALEXI), raw LPRM, and Noah CTRL (no assimilation) shows that averaged over the 3 months Noah exhibits the highest anomaly correlation with ΔUSDM (r = 0.61), followed by ESI (r = 0.55) and LPRM (r = 0.46). As expected, the assimilation of ESI and LPRM do in fact improve the anomaly correlations over the raw retrievals and the Noah Control simulation. The single assimilation of ESI and the dual assimilation (ALEXI ESI + LPRM) each exhibited the largest correlation with ΔUSDM (r = 0.65), while the single assimilation of LPRM (r = 0.62) was slightly lower, however significantly higher than the raw LPRM retrievals. This analysis will be expanded in Year 3 to include all proposed simulation methodologies (e.g., SM assimilation, near real-time GVF/albedo vs. climatological values) and include additional drought indicators.

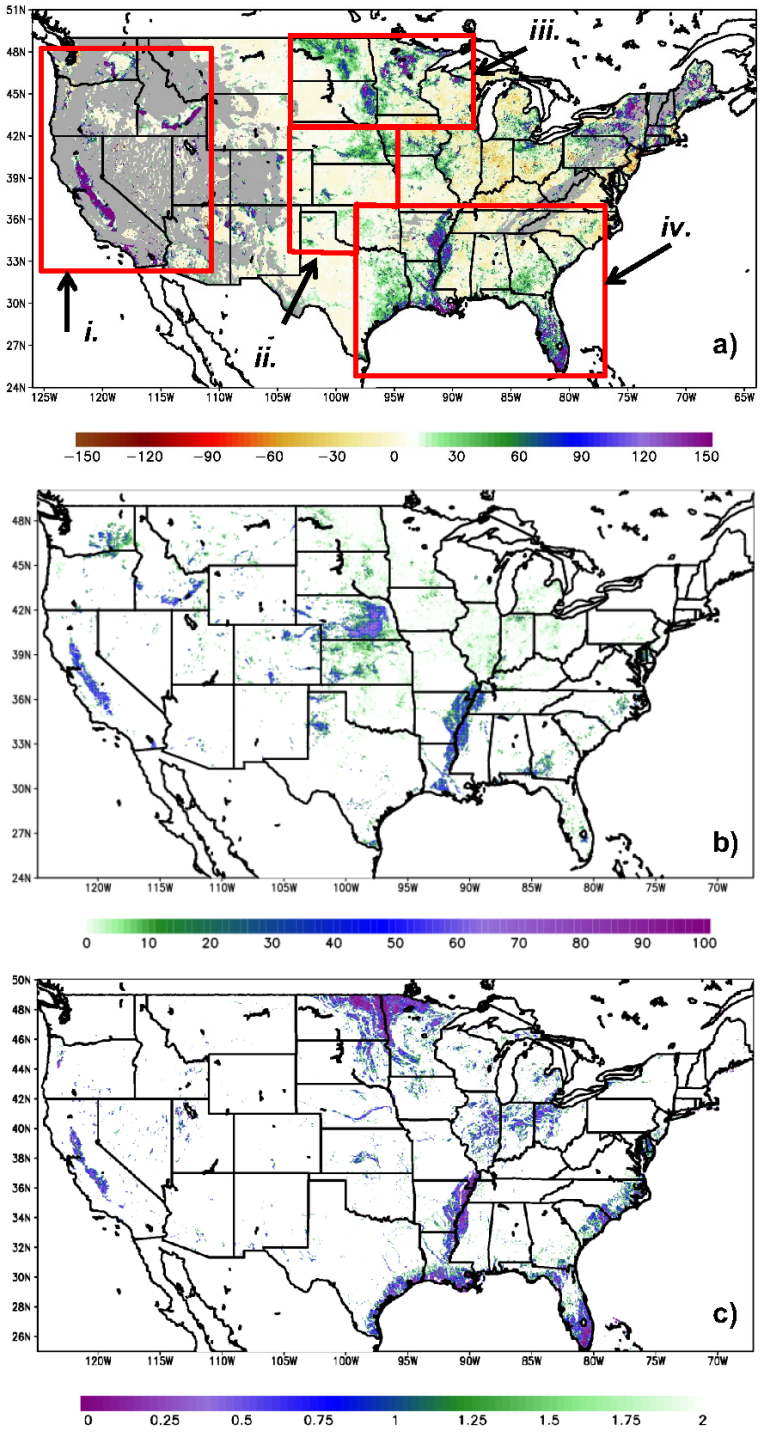

Fig. 6. a) ASSET (top) computed from an average of 13 JJA composites (2000-2012; Positive (negative) values indicate regions where ALEXI clear-sky LE was greater (less than) than Noah clear-sky LE, collocated with low annual variability of ALEXI clear-sky LE), b) simulated groundwater table depth (middle; Fan et al. 2007; Miguez-Macho et al. 2008) and c) MODIS irrigation percentage (bottom; Ozdogan and Gutman 2008).

Table 1. Spatial anomaly correlations computed against anomalies in the USDM drought classifications for June, July and August (2003-2011).

	ESI	LPRM	Noah	Noah+ESI	Noah+LPRM	Noah+ESI+LPRM
June	0.51	0.37	0.56	0.60	0.55	0.59
July	0.54	0.48	0.60	0.65	0.64	0.66
August	0.61	0.52	0.66	0.70	0.68	0.71
Mean	**0.55**	**0.46**	**0.61**	**0.65**	**0.62**	**0.65**

Fig. 7 shows an example of the merging through data assimilation of ALEXI ESI into the Noah LSM (version used in current operational NLDAS) for 5 August 2011. A large and significant drought was ongoing across the south central US during this analysis period. The merged ALEXI + NLDAS SM (Fig. 7c) anomaly map exhibited an increased correlation (r = 0.72) with the USDM classifications than either of the single products (Fig. 7. a-b; r = 0.64 and r = 0.68).

ii. ALEXI / ECV / Noah (2000-2014)

After the failure of AMSR-E in 2011, the assimilation experiments were repeated with the ESA ECV merged SM dataset and ALEXI over the 2000 to 2014 period. The results were similar to what was found in the initial analysis using LPRM, however, the ECV anomaly correlations were slightly higher than those found with LPRM. In general, the merged Noah and ESI product offered a higher upgrade than the merged Noah and ECV product. The merging of all three datasets (Noah+ESI+ECV) in the data assimilation system exhibited the highest increase of any of the single product anomaly correlations (r = 0.67).

Table 2. Spatial anomaly correlations computed against anomalies in the USDM drought classifications for June, July and August (2000-2014).

	ESI	ECV	Noah	Noah+ESI	Noah+ECV	Noah+ESI+ECV
June	0.54	0.49	0.60	0.60	0.56	0.61
July	0.57	0.48	0.61	0.67	0.66	0.68
August	0.61	0.51	0.63	0.70	0.65	0.72
Mean	**0.57**	**0.49**	**0.61**	**0.66**	**0.63**	**0.67**

Fig. 8-10 show examples of the US Drought Monitor classification and each product (ALEXI ESI, ECV and Noah) using the same D0-D4 percentile ranks as used in the USDM for 5 August 2007, 2008 and 2011. These maps will be available to users on the new NOAA STAR ESI website, supporting the GET-D system, in mid-2015. Providing anomaly and percentile maps of remotely sensed soil moisture products and NLDAS LSMs, along with products from a system that assimilates TIR and MW information into Noah will provide useful information to decision makers. Importantly, the three methods are largely independent, thus the merging of TIR, MW and modeling in a data assimilation system will add important information to current suite of drought indices than mainly rely on precipitation and vegetation information.

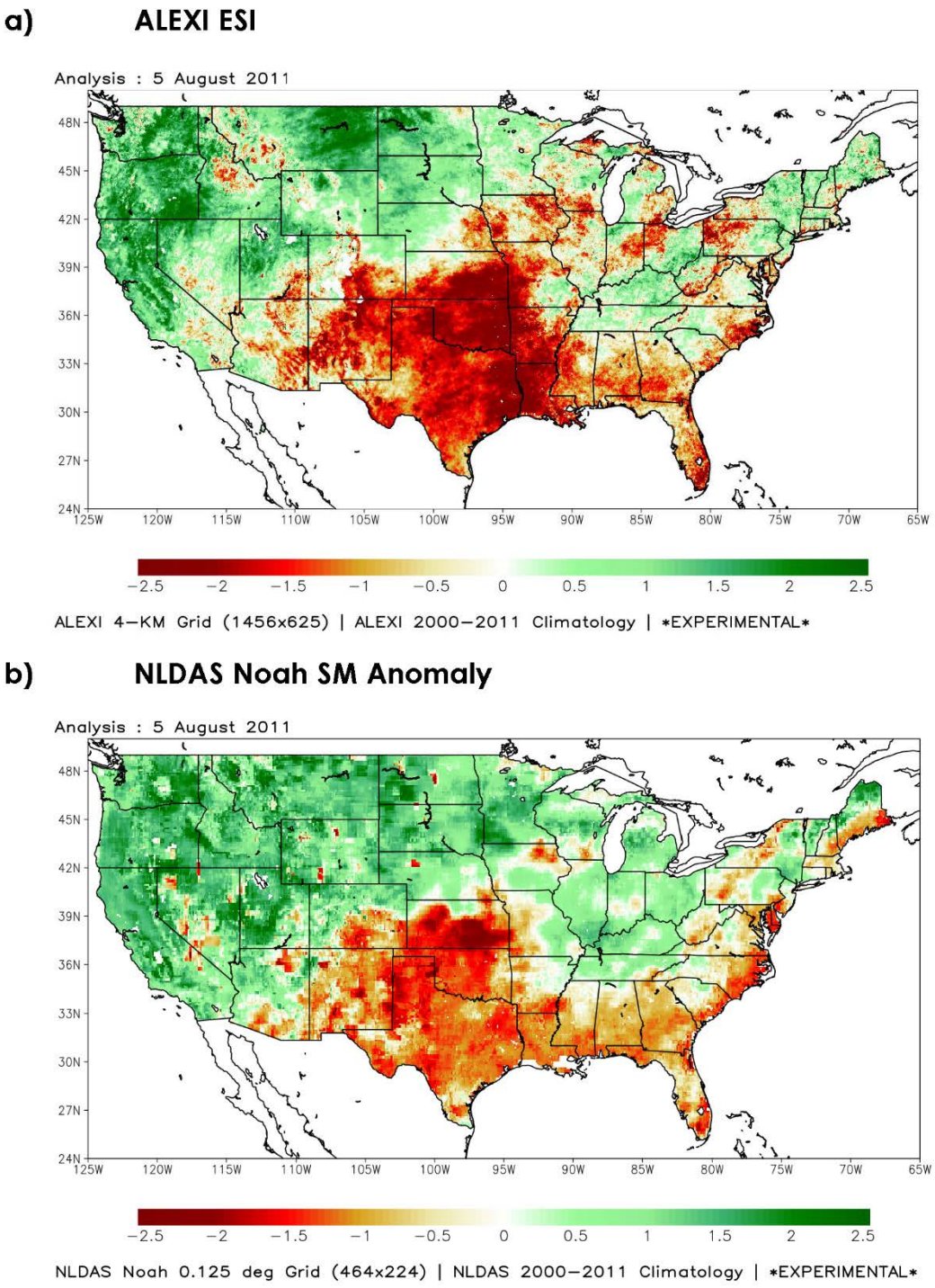

Fig. 7. Drought products valid on 5 August 2011 for a) ALEXI Evaporative Stress Index, b) open-loop simulation of Noah, c) merged ALEXI and NLDAS and d) U. S. Drought Monitor Drought Classifications.

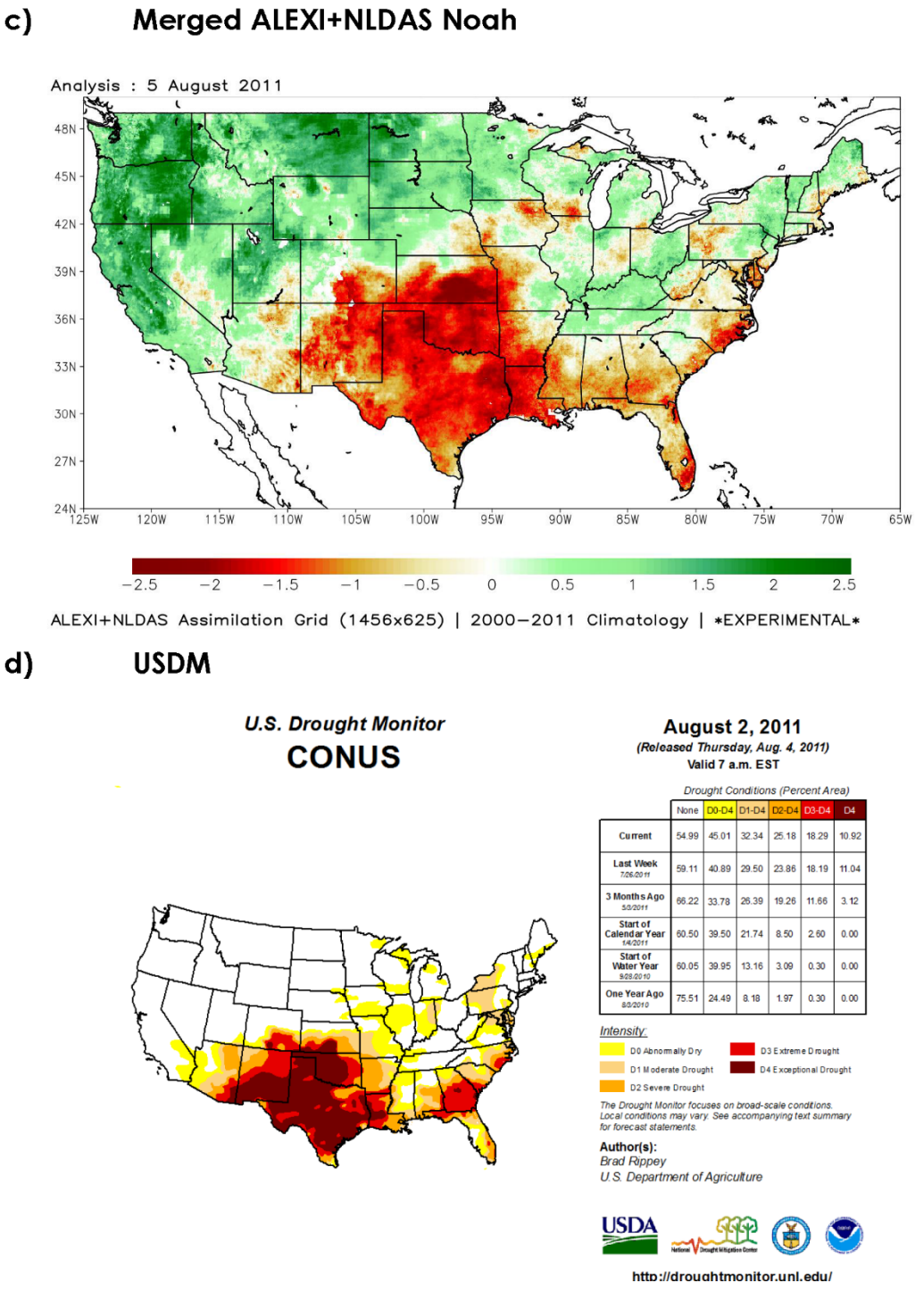

Fig. 7. Drought products valid on 5 August 2011 for a) ALEXI Evaporative Stress Index, b) open-loop simulation of Noah, c) merged ALEXI and NLDAS and d) U. S. Drought Monitor Drought Classifications.

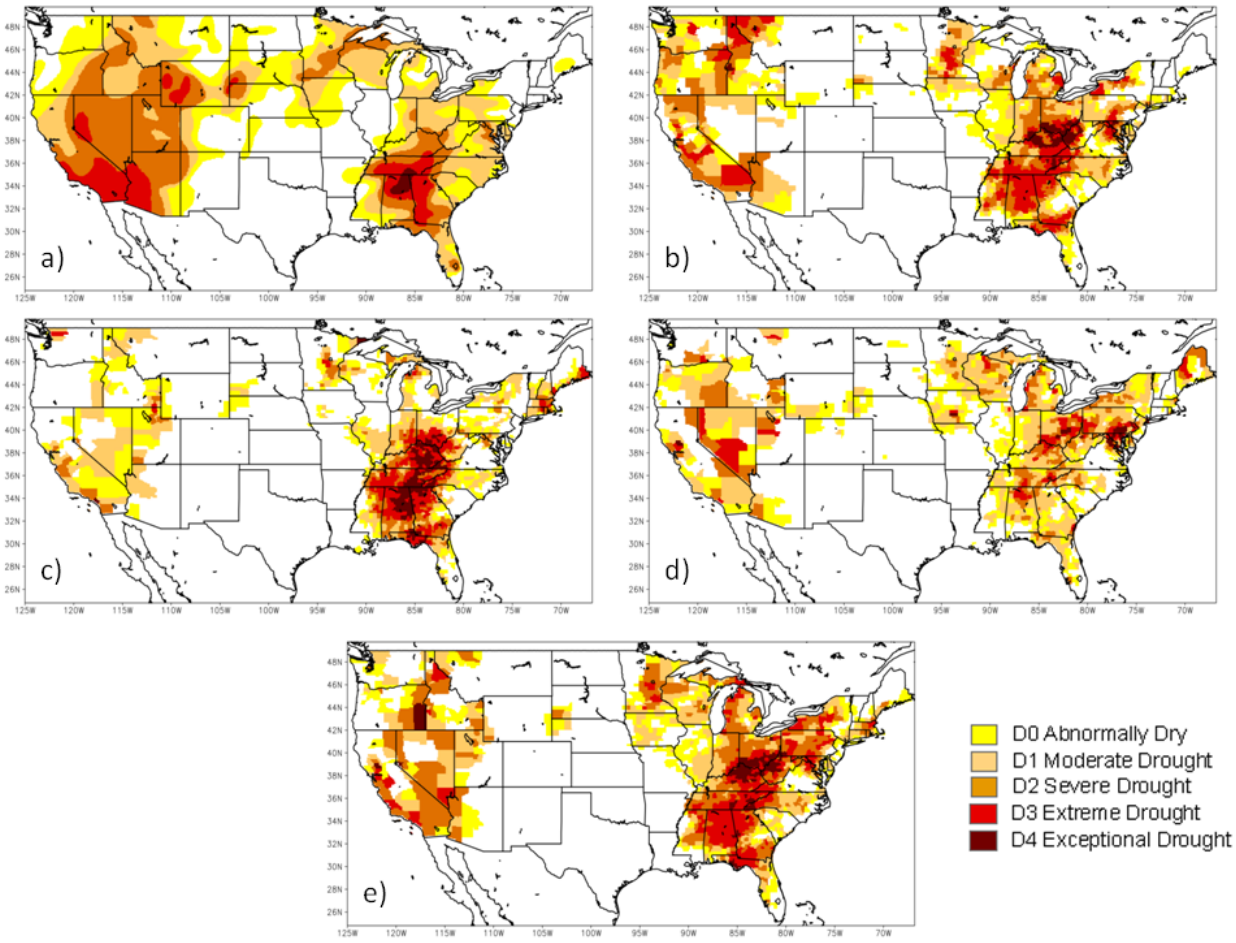

Fig. 8. United State Drought Monitor Classification (a), Noah SM drought analysis (b), ALEXI ESI drought analysis (c), ECV SM drought analysis (d) and merged data assimilation drought analysis (e) for 5 August 2007.

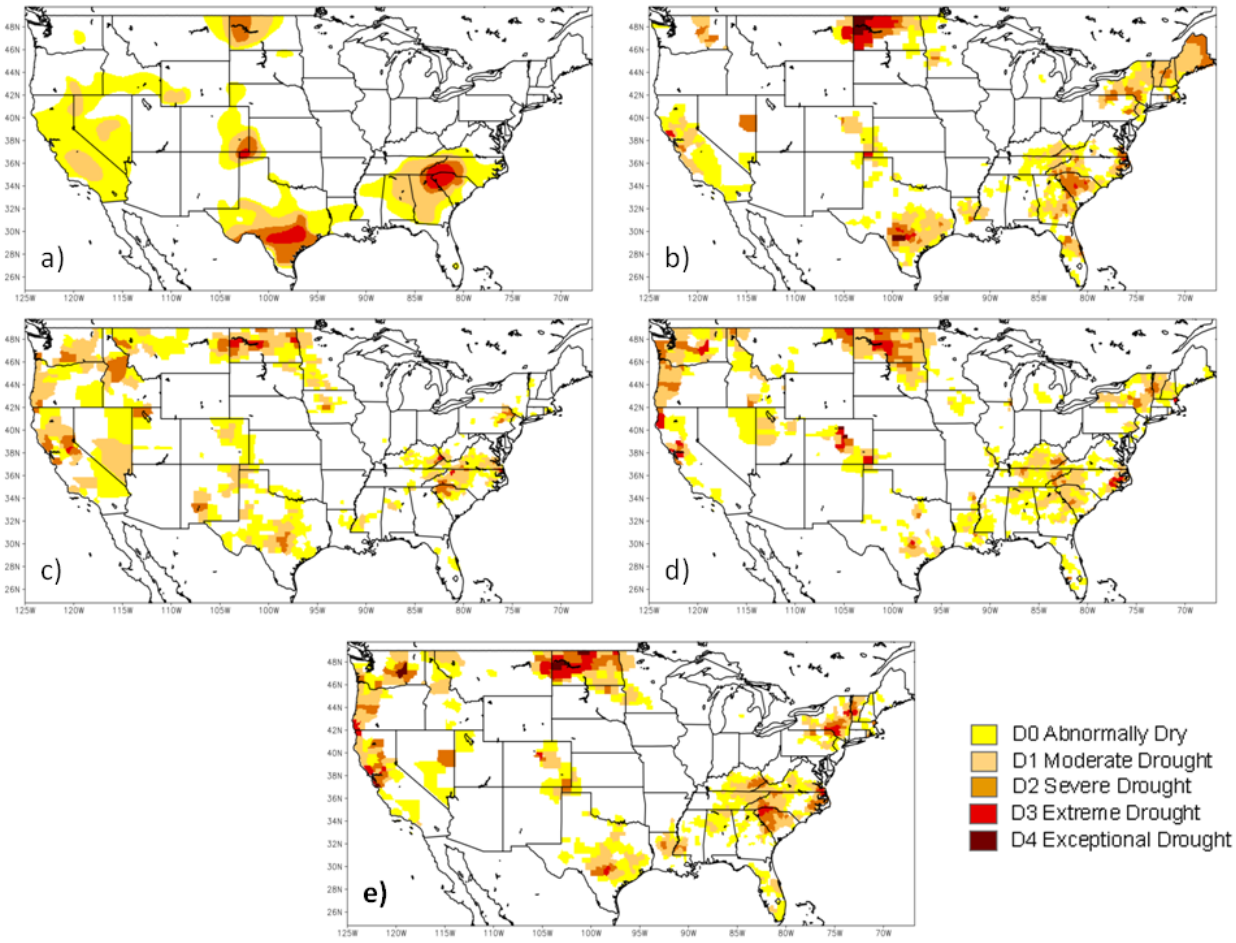

Fig. 9. United State Drought Monitor Classification (a), Noah SM drought analysis (b), ALEXI ESI drought analysis (c), ECV SM drought analysis (d) and merged data assimilation drought analysis (e) for 5 August 2087.

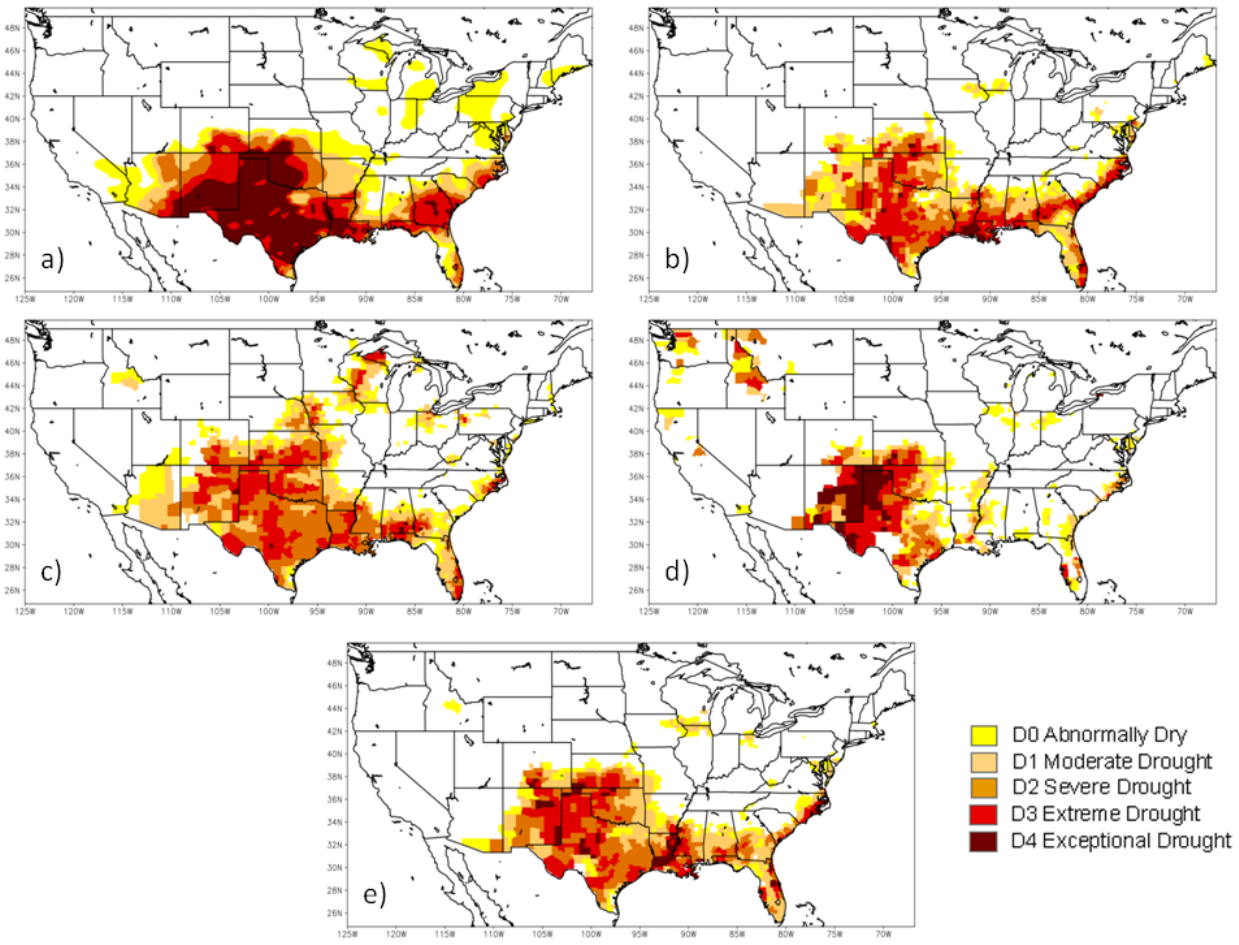

Fig 10. United State Drought Monitor Classification (a), Noah SM drought analysis (b), ALEXI ESI drought analysis (c), ECV SM drought analysis (d) and merged data assimilation drought analysis (e) for 5 August 2011.

e. Research-to-Operations (R2O) Plan and Outstanding Issues

The data assimilation system developed and evaluated during this project shows potential improvement for real-time drought monitoring using land surface modeling and remotely sensed observations of soil moisture from thermal infrared and microwave sensors. However, operational production of all the remotely-sensed soil moisture observations needed in the system is not currently available; however this work has been leveraged to fill this observational gap.

Our research team is currently beginning Year 2 of a project that will transition the production of ALEXI ESI into operations at the NOAA Office of Satellite and Product Operations (OSPO). Operational production is slated to begin in mid-2015. The system, GET-D (GOES Evapotranspiration and Drought Product System) will produce daily ET and ESI datasets from ALEXI over North America at a 10-km spatial resolution and CONUS at a 4-km spatial resolution. ***GET-D will be able to provide the operational support of a future ALEXI ESI / NLDAS data assimilation system.*** Also, our research team has developed and maintains an operational system at NOAA which produces near-real-time merged analysis of soil moisture from all available active and passive microwave sensors (SMOPS). The SMOPS system could potentially provide an operational stream of microwave products for the assimilation system but the use of SMOPS has been hampered by its relatively short period of record (2007-current), compared to ESA ECV. Retrospective processing back to 2000 (ESA ECV has been reprocessed back to 1978) is possible to match the ALEXI period of record. Our team is exploring potential funding avenues to support this work. While, the use of the ESA ECV product is optimal for retrospective analyses (as shown in this project), the ECV dataset is a "ESA Essential Climate Variable" and there are no current plans to operationally produce the product in near-real-time setting. This ultimately limits its use in a near-real-time assimilation-based drought monitoring system. ***SMOPS has the potential to provide the operation support of a future ALEXI ESI / Microwave / NLDAS data assimilation system, but is contingent on additional retrospective processing of the SMOPS system.*** NLDAS has begun operational production at NCEP EMC; however, the current system does not use any soil moisture assimilation. Our team will continue to work with the EMC group to move towards implementing TIR and MW SM assimilation into the operational NLDAS system.

The development of ALEXI ESI facilitated by this project has also lead to additional data assimilation activities with NCEP EMC. For example, our research team has begun work on a NOAA-funded project to assimilate ALEXI datasets in the North American Mesocale (NAM) model at EMC. This work will assess the impact of assimilating ALEXI information in a mesoscale number weather prediction (NWP) model towards improving weather forecasts. Additionally, the assimilation MW soil moisture information from SMOPS is being tested in the Global Forecast System (GFS) at EMC. An initial analysis of the impact of SMOPS data assimilation in the GFS showed improvements in the forecasts of precipitation. Improvements to forecasts from NAM and GFS/CFS have the potential to have significant impacts to 0-15 day forecasts of precipitation which are important to the monitoring on current and developing drought conditions on those time scales.

3) End-User Interaction / Data Product Dissemination

A website (hrsl.arsusda.gov/drought) has been developed at HRSL to visualize ESI products side-by-side in comparison with USDM drought classifications and other drought indicators, both in real-time and retrospectively. End-user feedback and associated web page modifications are being recorded using a SharePoint collaboration web page, which can be accessed by the PI and web developers. Feedback provided by users Mark Svoboda (NDMC) and Kingste Mo (CPC) regarding access speed, annotation, and documentation has been used to improve web delivery. Under recommendations from USDM, an ESI change product was added to the website, to highlight areas of rapidly changing conditions. A link to this page has been established through the NIDIS Drought Portal at: http://www.drought.gov/drought/content/products-current-drought-and-monitoring-remote-sensing/evaporative-stress-index.

An additional website (mirrored with USDA HRSL) is currently under development at NESDIS STAR which will provide products currently disseminated at the USDA HRSL. Additional products developed from the data assimilation system in this project will also be available, initially for retrospective periods. A near-real-time production of the assimilation-based products will depend on leveraging future funding to support those activities. An integration of the data assimilation system into the GET-D framework is currently being explored.

ESI products were evaluated in relation to NASS crop yield datasets over the ESI climatological period. Currently, NASS yield forecasts, released starting in August, are driven by correlations with NDVI from various sensors and LST from MODIS. Fundamentally, ESI should be able to effectively integrate signals conveyed by NDVI and LST, as well as precipitation deficits, and has potential to add value to current estimation algorithms used by NASS. Collaborator D. Johnson at NASS completed a preliminary evaluation of ESI correlations with USDA corn and soybean yields over the 2000-2012 period. Correlations at state scale are maximized for corn in early August, coinciding with the first NASS yield forecast issued effective August 1 (Fig 11). Crops in AR are largely irrigated, and may show weaker ET-based signals, while poor correlations in MN and ND require further investigation. Based on these results, NASS plans to implement ESI-based yield estimates in August 2013 for internal comparison with standard forecasts. However, NASS collaborators have indicated interest in higher resolution ESI products to better discriminate between crops and other land-use types, potentially improving the results found with the 10-km ESI products (Fig. 11).

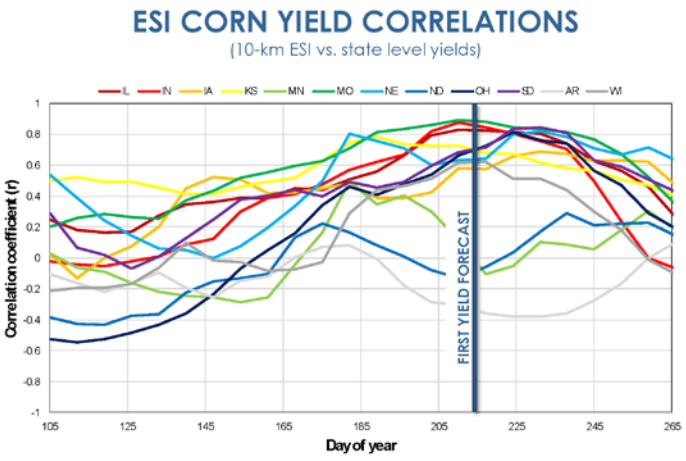

Figure 11. Correlations between 10-km ESI aggregated to state scale and final USDA state-level yield estimates for major corn-producing states.

4) Publications (Published and In Preparation/Under Review)

Anderson, M. C., C. R. Hain, J. A. Otkin, X. Zhan, K. Mo, M. Svoboda, B. Wardlow, and A. Pimstein, 2013: An Intercomparison of Drought Indicators Based on Thermal Remote Sensing and NLDAS-2 Simulations with U.S. Drought Monitor Classifications. *J. Hydrometeor*, **14**, 1035–1056. doi: http://dx.doi.org/10.1175/JHM-D-12-0140.1

Fang, L., C. R. Hain, X. Zhan and M. C. Anderson, 2014: Intercomparison and validation of soil moisture estimates from microwave and thermal infrared remote sensing and land surface modeling. *To be submitted to J. Hydrometeor*.

Fang, L., C. R. Hain, X. Zhan and J. Yin, 2014: Impact of near-real-time satellite observations of solar insolation, green vegetation fraction and albedo on soil moisture estimates from the Noah land surface model. *To be submitted to J. Hydrometeor.*

Hain, C. R., W. T. Crow, J. R. Mecikalski, and M. C. Anderson, 2012: Developing a dual assimilation approach for thermal infrared and passive microwave soil moisture retrievals, *Water Resour. Res.*, **48**, W11517, doi:10.1029/2011WR011268.

Hain, C. R., W. T. Crow, M. C. Anderson and M. T. Yilmaz, 2014: Diagnosing neglected soil moisture sources/sink processes via a thermal infrared-based two-source energy balance model, *Submitted to J. Hydrometeor*.

Otkin, J. A., M. C. Anderson, C. R. Hain, and M. Svoboda, 2014: Examining the Relationship between Drought Development and Rapid Changes in the Evaporative Stress Index. *J. Hydrometeor*, **15**, 938–956. doi: http://dx.doi.org/10.1175/JHM-D-13-0110.1.

Otkin, J. A., M. C. Anderson, C. R. Hain and M. Svoboda, 2014: Using temporal changes in drought indices to generate probabilistic drought intensification forecasts, *J. Hydrometeor*., *In Press*.

5) References

Fan, Y., G. Miguez-Macho, C. P. Weaver, R. Walko, and A. Robock, 2007: Incorporating water table dynamics in climate modeling: 1. Water table observations and equilibrium water table simulations, *J. Geophys. Res*. **112**, D10125, doi:10.1029/2006JD008111.

Miguez-Macho, G., H. Li, and Y. Fan, 2008: Simulated Water Table and Soil Moisture Climatology Over North America. *Bull. Amer. Meteor. Soc.*, **89**, 663–672.

Ozdogan, M., and G. Gutman, 2008: A new methodology to map irrigated areas using multi-temporal MODIS and ancillary data: An application example in the continental US. *Remote Sens. Environ.*, **112**, 3520-3537.